2024 IEEE International Symposium on Antennas and Propagation and INC/USNC-URSI Radio Science Meeting (AP-S/INC-USNC-URSI) | 979-8-3503-6990-8/24/$31.00 ©2024 IEEE | DOI: 10.1109/AP-S/INC-USNC-URSI52054.2024.10686912

Exploring the Potential of Quasi-Conformal Transformed Luneburg Lens for Imaging Applications

Habeeb F. Adeagbo(1), and Binbin Yang (1)
(1) North Carolina A&T State University, Greensboro, NC, 27411, USA (byang1@ncat.edu)

***Abstract*—This paper demonstrates the prospects of using a Modified 3D Spherical Luneburg lens antenna for imaging. The proposed imaging experimental setup comprises the lens fed by a rectangular waveguide to shine directive beams on the targets of different shapes placed in the path of the beams. The 60 mm diameter lens with a maximum directivity of 17 dBi is enclosed in a 160 mm diameter spherical Perfectly Matched Layer. Single-frequency monostatic full-wave simulations were performed at 18 GHz. The scattering parameters and the simulated far-field data are fed to the imaging algorithm based on truncated singular value decomposition, and the reconstructed images show the imaging capabilities of a Quasi-Conformal Transformed Luneburg lens.**

I. Introduction

A Luneburg lens is a highly directive spherical dielectric GRadient INdex (GRIN) lens with a high radiation efficiency and a symmetrically varying relative permittivity which decreases radially from the center to the outside surface of the lens[1]. Luneburg lens antennas are an important type of ultra-wideband (UWB) antennas at microwave and millimeter wave frequencies. In the existing literature, unlike most of its UWB antenna counterparts such as Vivaldi and bow-tie antennas used for high-resolution imaging, Luneburg lens mostly finds applications in wireless communications and acoustic systems. Exploring the Luneburg lens' imaging capabilities could open new doors for its applications in microwave imaging which would in turn make the lens useful for short-range imaging applications such as biomedical imaging, through-the-wall imaging, concealed weapon detection, and long-range imaging applications such as radar, remote sensing, and underground surveillance.

Transformation Optics (TO) theory allows us to modify the geometry of a Luneburg lens while still retaining the electromagnetic properties of the default spherical Luneburg lens. Flattening one side of the lens using TO theory makes it easier to incorporate planar waveguides/array of feeds for low-cost beamforming[2]. Microwave imaging techniques leverage these beamforming devices to shine highly directive beams upon targets. The image of the target objects can be reconstructed based on scattered waves received by the imaging devices after being processed by an imaging algorithm.

In this paper, we present a modified Luneburg lens imaging system, an advancement on our prior work reported in [3]. Image reconstruction is achieved by using an imaging algorithm based on truncated singular value decomposition.

II. Imaging System Setups

The imaging system consists of two simulation setups; the setup with targets (shown in Fig. 1.) and the setup without targets; both of the same system size, lens and waveguide size, and position. The targets are dielectric materials of higher relative permittivity values when compared with the permittivity of the surrounding environment. The targets are placed in the path of the beams, achieved by placing the rectangular waveguide feeds at different locations on the flat side of the Luneburg lens to form an array-like feed position map.

The parameters of the Luneburg lens used in the system are described comprehensively in [3]. The imaging system's geometric entity and material properties assignment were done putting in mind the possibilities of physical realization with 3D printing technology. We carried out a full-wave simulation using a frequency domain EM solver at 18 GHz. Antenna beam steering was achieved by parameterizing the rectangular waveguide positions making it possible to scan the targets from different waveguide locations. The scattering parameters at the 81 waveguide positions and the far-field radiation pattern data are saved for target image reconstruction.

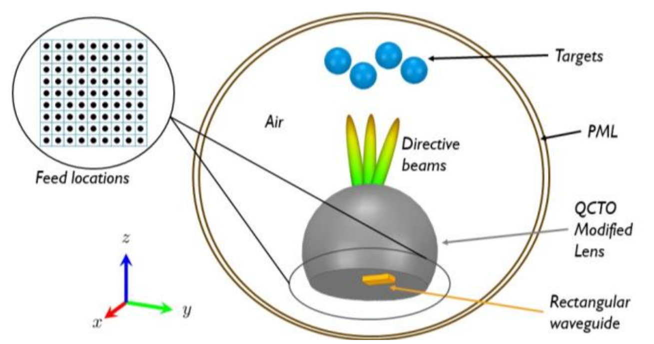

Figure 1. The QCTO Modified Spherical Luneburg Lens imaging system with spherical targets

III. Formulation of the Imaging Algorithm

Under the Born Approximation, the scattered electric field at the waveguide positions can be expressed as

$$E_s(r,k) = k^2 \int_v G(r,r',k) E_{inc}(r',k) \chi(r')\, dr' \qquad (1)$$

where r is the waveguide position, r' is the target position, k is the wavenumber in free space. $G(r,r',k)$ is the Green's function, $E_{inc}(r', k)$ is the incident field at the target position and $\chi(r')$ is the contrast function[4].

Applying the reciprocity principle to equation (1), Green's function is equal to the incident field[4]. Therefore,

$$E_s(r,k) = \int_v E_{inc}{}^2(r',k)[k_t^2(r') - k_0^2]\, dr' \qquad (2)$$

where k_0 is the wave number of the background medium and k_t is the wave number of the targets.

For image reconstruction, the scattered field at the waveguide positions can be simplified in relation to our imaging setups with and without targets. Considering the waveguide open end for both setups, the scattered field at the waveguide positions can be related to the scattering parameters at all feed positions.

$$\frac{E_S(r,k)}{E_0} \equiv S_{11}^{w} - S_{11}^{w/o} \equiv \Delta S_{11} \qquad (3)$$

where E_0 is the incident field at the open end of the waveguide and is assumed to be 1, S_{11}^{w} is the measured Scattering parameters for the setup with the targets, and where $S_{11}^{w/o}$ is the measured Scattering parameters for the setup without the targets.

Therefore, equation (2) becomes:

$$\Delta S_{11} = \int_v E_{inc}{}^2(r',k)[k_t^2(r') - k_0^2]\, dr' \qquad (4)$$

The volume integral in equation (4) can be approximated to summations, and the square of the incident field (which is also proportional to E_0) is the radiation power pattern of the antenna.

$$\Delta S_{11} = \sum_{p=1}^{P} \sum_{m=1}^{M} \sum_{n=1}^{N} P(\theta, \emptyset) \exp(-j2kr)\, [k_t^2(r') - k_0^2] \qquad (5)$$

where $(r, \theta, \emptyset)$ is the spherical coordinates of the target positions. $P(\theta, \emptyset)$ is the radiation power pattern, p is the number of waveguide positions, m is the number of elevation angles θ and n is the number of azimuth angles $\emptyset$ specified in the radiation pattern measurement.

The ΔS_{11} and radiation pattern matrices are obtained from the simulation or measurements, equation (5) can be expressed in the matrix form as:

$$S = Hg \qquad (6)$$

where S is the vector of the scattering parameters difference, H is the system response matrix represented by the radiation pattern matrix, and g is the vector of reflectivity coefficients of the targets.

Equation (6) is an underdetermined linear system equation, and there are various methods to solve it. In this work, we used the truncated singular value decomposition method to solve it for image reconstruction.

IV. RESULTS

We carried out the imaging experiment using two sets of targets. Experiment A consists of four spherical targets of 5 mm radius located at (±25, ±25). Experiment B consists of two 50 mm long rectangular bars located at (0, ±25). Fig. 2 shows the 2D ground truth of the targets in both experiments.

A total of 9×9 feed positions were reshaped to give an 81×1 S vector. The number of elevation angles θ and azimuth angles $\emptyset$ used in the full-wave simulation are 30 and 120 respectively resulting in a 81×3630 system response matrix.

Fig. 3 shows the imaging result of the two experiments using the proposed Luneburg lens imaging system and the truncated singular value decomposition algorithm. The reconstructed images show the exact locations of the targets. While the image reconstruction is not flawless, it is still possible to identify and differentiate between the targets. This illustration demonstrates the viability of the imaging system.

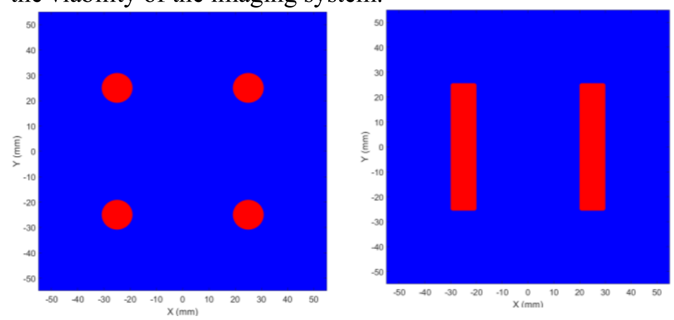

(a) (b)

Figure 2. The 2D Ground truth of (a) 4 spherical targets and (b) two rectangular bar targets.

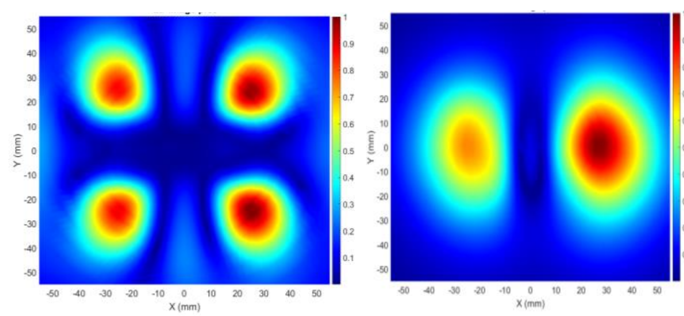

(a) (b)

Figure 3. The 2D reconstructed image of (a) 4 spherical targets and (b) two rectangular bar targets.

V. CONCLUSION

This paper investigates a Modified Luneburg Lens imaging system and the imaging algorithm based on truncated singular value decomposition. The imaging results prove the viability of using a modified Luneburg lens for imaging applications.

ACKNOWLEDGMENT

This material is based upon work supported by the National Science Foundation under Grant No. 2138741.

REFERENCES

[1] R. K. Luneburg and M. Herzberger, "Mathematical theory of optics," *Univ. of California Press, 1964.*

[2] B. Yang, Y. Oh, X. Hu and J. J. Adams, "Implementation of A Flat-Bottom Luneburg Lens Based on Conformal Transformation Optics," in *2021 IEEE MTT-S Int. Microwave Symp. (IMS), Atlanta, GA, USA, 2021, pp. 556-559.*

[3] H. F. Adeagbo, B. Yang "Microwave Imaging using Quasi-Conformal Transformed Luneburg Lens," in *Proc. Int. Symp. Antennas Propag.*, Oregon, US, Jul. 2023, pp. 469–470.

[4] Q. Cheng, A. Alomainy, Y. Hao, "Luneburg Lens Imaging with Compressive Sensing," in *2017 Sixth Asia-Pacific Conference on Antennas and Propag. (APCAP), Xi'an, China, 2017, pp. 1-3.*